Geomorphology 272 (2016) 127–136

Contents lists available at ScienceDirect

Geomorphology

journal homepage: www.elsevier.com/locate/geomorph

Circulation patterns related to debris-flow triggering in the Zermatt valley in current and future climates

Floor van den Heuvel [a,*], Stéphane Goyette [b], Kazi Rahman [a], Markus Stoffel [b,c,d]

[a] University of Geneva, Institute for Environmental Sciences, 66 Boulevard Carl-Vogt, 1205, Geneva, Switzerland
[b] Climatic Change and Climate Impacts (C3i), Institute for Environmental Sciences, 66 Boulevard Carl-Vogt, 1205, Geneva, Switzerland
[c] Department of Earth and Environmental Sciences, University of Geneva, 13 rue des Maraîchers, 1205, Geneva, Switzerland
[d] dendrolab.ch, Institute of Geological Sciences, University of Bern, Baltzerstrasse 1 +3, 3012, Bern, Switzerland

ARTICLE INFO

Article history:
Received 15 June 2015
Received in revised form 10 December 2015
Accepted 15 December 2015
Available online 14 February 2016

Keywords:
Debris flows
Climate change
Extreme precipitation
Zermatt valley

ABSTRACT

The principal objective of this study was to investigate the types of large-scale meteorological situations that are conducive to the precipitation and temperature conditions most likely to trigger debris flows in the Zermatt valley, Switzerland, under current and future climates. A two-dimensional Bayesian probability calculation was applied to take account of uncertainties in debris-flow triggering. Precipitation quantities exceeding the 95th percentile of daily precipitation amounts were found to have a significantly higher probability to coincide with observed debris flows. A different relationship exists for extreme temperatures, however. Southerly air flows, weak horizontal pressure gradients over Europe, and westerly flows are mostly associated with observed debris flows and 95th precipitation percentile exceedances. These principal flow directions are well represented in the regional climate model (RCM) HIRHAM control simulations for events exceeding the 95th precipitation percentile and the 30th temperature percentile. Under the IPCC A2 emission scenario, westerly and southerly flows are mostly responsible for these precipitation and temperature conditions under the hypothesis of slow adaptation to climate change (HS1/HC1). Under the hypothesis of rapid adaptation to climate change (HS1/HS1), southerly flows and weak horizontal pressure gradients are likely to gain in importance. In both scenarios for the future, southeasterly flows are among the principal flow directions responsible for the joint exceedance of the 95th precipitation percentile and the 30th temperature percentile, while these were absent in observations and the control simulation.

1. Introduction

Debris flows are a phenomenon typical of steep torrential catchments and are formed by a mixture of water, fine sediment, boulders, and vegetation (Jakob and Hungr, 2005; Borga et al., 2014); they typically occur during (extreme) rainfall events and/or the sudden release of large amounts of water and therefore form one of the more common geomorphic processes in mountain areas worldwide, including the Swiss Alps (Stoffel et al., 2014a). As a result of the high velocities and considerable energies involved in debris flows, they repeatedly cause casualties as well as considerable damage to infrastructure (Jonkman, 2005; Jakob et al., 2011; Stoffel et al., 2011; Borga et al., 2014). Although many site-specific factors may influence debris-flow triggering, rainfall quantities and intensity as well as rising mean and extreme air temperatures have been identified as the most prominent triggers in various debris-flow catchments in the Swiss Alps (Wieczorek and Glade, 2005; Schneuwly-Bollschweiler and Stoffel, 2012; Stoffel et al., 2014a, 2014b). Soil saturation leads to increased shear forces as well as surface water flow that in turn leads to erosion and debris-flow triggering, especially when pore saturation happens at potential rupture surfaces (Sassa, 1984; Iverson et al., 1997). This is particularly the case for the study area, where scree slopes can hold very little quantities of water. Furthermore, Schneuwly-Bollschweiler and Stoffel (2012) found that high temperatures are significantly correlated with debris-flow occurrence. The reason for this is that higher temperatures may lead to rainfall instead of snowfall as warmer air can contain more water vapour, according to the Clausius–Clapeyron equation, and ensuing condensed moisture would ultimately be transferred into the ground.

Observations during the twentieth century and climate model simulations of future climate change indicate that important changes in these variables may be expected (Pall et al., 2007; Gobiet et al., 2014). Depending on the emission scenario, climate models project changes in the mean global surface temperature to exceed the 1850–1900 average by 1.5 to 2 °C at the end of the twenty-first century according to the Intergovernmental Panel on Climate Change (IPCC, 2013). At higher elevations, such as in the Swiss Alps, this temperature rise may be exacerbated (Beniston et al., 2003; Gobiet et al., 2014). The IPCC (2013) also mentions that the frequency and intensity of heavy precipitation events have likely increased in Europe since 1950. Furthermore, regional climate models (RCMs) point to an expected decrease in mean summer precipitation in the Alps as well as a decrease in the frequency of extreme precipitation

* Corresponding author.
E-mail address: floortje.vandenheuvel@epfl.ch (F. van den Heuvel).

http://dx.doi.org/10.1016/j.geomorph.2015.12.010
0169-555X/

events for this season (Beniston et al., 2007; Christensen and Christensen, 2007; Rajczak et al., 2013; Gobiet et al., 2014). However, the precipitation quantities during future extreme precipitation events may well be on the rise (Christensen and Christensen, 2003; Emori and Brown, 2005; Kharin et al., 2007; Pall et al., 2007; Lenderink and van Meijgaard, 2008; Kyselý and Beranovà, 2009; IPCC, 2012; Rajczak et al., 2013) though important differences and large uncertainties exist at the local scale (Fischer et al., 2013). It is further estimated that changes in precipitation patterns and quantities are the result of an intensification of the hydrological cycle with climate warming (Schär et al., 1999; Seneviratne et al., 2006).

Important differences exist in the response of debris flows to climate change in debris-limited areas or in transport-limited areas (Jakob, 1996). In debris-limited areas, a reduction in the number of freezing days as well as a shift in the 0 °C isotherm to higher elevations will reduce the surface affected by weathering and likely result in a decrease in debris-flow activity (Jomelli et al., 2009). Though at higher altitudes, increase in freeze-thaw cycles could also liberate greater quantities of debris. However, in transport-limited areas, such as the periglacial environments of this study, debris-flow frequency is not limited by sediment availability but by climatic variables (Stoffel and Beniston, 2006; Stoffel, 2010; Lugon and Stoffel, 2010). Changes in these variables have caused permafrost thawing, reduced snow cover, and the earlier occurrence of effective rainstorms that in turn have led to an observed extension of the debris-flow season. In several catchments of the Zermatt valley, debris flows now occur between May and October, whereas their occurrence was limited to from June through September until recently (Bollschweiler and Stoffel, 2010a; Schneuwly-Bollschweiler and Stoffel, 2012). Debris-flow frequency in this area is expected to change little by the mid-twenty-first century, but increased sediment availability (as a result of accelerated permafrost thawing) and an increase in extreme 1-day precipitation events between July and October may lead to debris flows of greater magnitudes (Stoffel et al., 2014b). Higher temperatures could further extend the debris-flow season into April and November. For the second part of the twenty-first century, studies indicate a shift in debris-flow triggering rainstorms from July and August toward spring and autumn (Stoffel et al., 2014b). Early in the season, small rainfall quantities can lead to small debris flows as a result of rain-on-snow effects and the presence of seasonal ice cementing loose debris at shallow depth, thereby reducing the quantity of debris available for erosion to the top layer next to the surface (Stoffel et al., 2011; Stoffel and Huggel, 2012). In fall, as a result of permafrost thawing in the source areas of debris flows during summer, more material can be mobilised by debris flows from the permafrost bodies, but larger precipitation quantities will be needed for debris-flows to be triggered (Stoffel et al., 2011; Stoffel and Huggel, 2012). Stratiform rainfall, which typically occurs between August and October under current climatic conditions (Stoffel et al., 2005), can lead to the (partial) failure of the active layer of the permafrost body and consequently results in debris flows of large magnitudes (Stoffel et al., 2011).

The shift in the seasonality of debris-flow triggering rainstorms as described above could likely lead to a diminution in the overall debris-flow frequency in the Zermatt valley, as summer debris-flow events are supposed to become less frequent (Stoffel, 2010; Stoffel et al., 2014b). However, this reduction in debris-flow frequency is expected to cause important sediment accumulations that in turn could produce debris flows of even larger magnitudes than observed in the past during stratiform rainstorms in autumn (which are projected to be more common by 2100) (Stoffel and Beniston, 2006; Stoffel, 2010; Stoffel et al., 2014b).

As precipitation and temperature are not the only variables involved in debris-flow triggering and because of local characteristics and uncertainties related to the scenario-driven climate model projections, some degree of uncertainty exists in the prediction of debris-flow events. This study therefore seeks to take into account this measure of uncertainty by attributing probabilities to the coincidence of joint exceedances of precipitation and temperature percentiles with observed debris flows.

Several studies have linked large-scale pressure distributions to heavy precipitation events over Europe (Qian et al., 2000), in the eastern Italian Alps (Nikolopoulos et al., 2015), in Switzerland (Courvoisier, 1981), and in the Valais region (Attinger and Fallot, 2003), with one study even focusing specifically on large-scale meteorological situations during observed debris-flow events in the Zermatt valley (Toreti et al., 2013). Situations with an atmospheric-pressure trough over western Europe or situations corresponding to a low pressure system to the west (over the Bay of Biscay) correspond to observed debris flows and heavy precipitation events in the Alps (Attinger and Fallot, 2003; Toreti et al., 2013). To these should be added synoptic situations causing westerly to northwesterly flows and weak horizontal pressure gradients over Europe (Courvoisier, 1981). Quite similar synoptic situations have been related to debris-flow triggering in the eastern Italian Alps by Nikolopoulos et al. (2015). Indeed, the relationship between large-scale mean sea level pressure (MSLP) fields and heavy precipitation is well-established. At the same time, climate models appear to represent these pressure fields and atmospheric circulation types in an appropriate manner (Rohrer, 2013). This study thus also investigates on how the large-scale MSLP situations conducive to the precipitation and temperature conditions most likely to trigger debris flows might evolve in a future climate.

2. Materials and methods

2.1. Data

For this study we used a database containing the dates of 119 reconstructed debris-flow events in the Zermatt valley covering the period 1864–2008 (Bollschweiler and Stoffel, 2010a). In their study, Schneuwly-Bollschweiler and Stoffel (2012) dated injuries caused to trees by debris flows with up to monthly precision using archival records and dendrogeomorphic techniques (Bollschweiler and Stoffel, 2010b; Stoffel and Corona, 2014). The coupling of these records with meteorological records from three meteorological stations in the area as well as data from the river gauging stations allowed the identification of debris-flow triggering rainstorms. As the Zermatt valley is a relatively dry area where the annual mean precipitation at Zermatt is 639 mm and that of Grächen is 653 mm over the period 1981–2000 (source: MeteoSwiss), the number of events where precipitation is over 10 mm and temperature greater than 5 °C are scarce and thus allow attribution of individual rainstorms to triggered debris flows (Schneuwly-Bollschweiler and Stoffel, 2012). Fig. 1 illustrates the time series and the months on which debris flows were identified.

Observed daily mean temperature and daily precipitation sums were taken from the Zermatt station (46°01′ N, 7°45′ E at 1638 m asl) and the Grächen station (46°11′ N, 7°49′ E at 1619 m asl), with the latter extending back to 1864. Because of the high correlation between the meteorological data of the two stations and the years of missing data at the meteorological station of Zermatt, the station in Grächen was used as a reference station for this study. For example, the linear correlation coefficient for daily precipitation totals for these two stations for the period (1959–2014) is $r = 0.86$ (source: MeteoSwiss).

Daily mean temperature, MSLP values, and daily precipitation from the control simulation (HC1) and future period (HS1) were obtained from the HIRHAM model of the Danish Meteorological Institute (DMI) run in the context of the EU-FP5 research programme PRUDENCE (Christensen, 2004). The simulation for the future period was run using the IPCC A2 emission scenario. The grid point closest to Zermatt with an altitude of 2230 m was chosen and is located ca. 10 km away from the study area. The MSLP data for the entire HIRHAM grid and for the specific events corresponding to the joint exceedance of the precipitation and temperature percentiles of interest have been first selected from the PRUDENCE data.

2.2. Probability calculation

For the observed data, precipitation and temperature quantiles were calculated over the period 1864–2008 for the debris-flow season defined as 1 May to 31 October (Stoffel et al., 2008, 2011, 2014a). For the

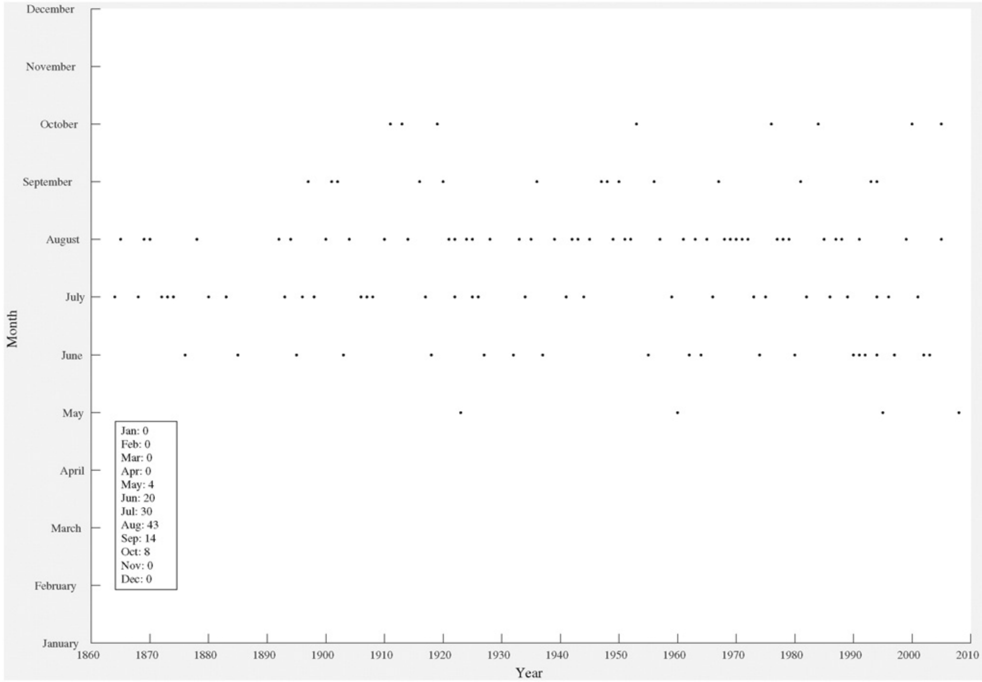

Fig. 1. Time series of debris-flow occurrence in the Zermatt valley.

simulated data, precipitation and temperature percentiles were calculated over the control (1961–1990) and future (2071–2100) periods, and the use of joint quantiles of precipitation and temperature was done similarly as in Beniston and Goyette (2007) and Beniston (2009). Probabilities were then calculated applying the two-dimensional Bayesian approach on observed data as described by Berti et al. (2012) in their study on landslides. Bayesian methodology is based on the updating of the prior probability $P(A)$ (in this case the probability of a debris flow occurring in the study area) with relevant data (i.e., precipitation and temperature data) resulting in a posterior probability $P(A|B,C)$ (the probability of a landslide occurring given certain precipitation and temperature conditions). As such, the Bayesian method allows the evaluation of the significance of the variable(s) in question as well as the uncertainty arising from the complex mechanisms behind debris-flow triggering. The conditional probability that a debris flow A occurs during a certain extreme rainfall event of magnitude B and a temperature event of magnitude C is given by Eq. (1) (adapted from their Eqs. (1) and (3)).

$$P(A|B,C) = \frac{P(B,C|A) * P(A)}{P(B,C)} \approx \frac{\left(N_{(B,C|A)} \div N_A\right) * \left(N_A \div N_R\right)}{\left(N_{B,C} \div N_R\right)} \approx \frac{N_{(B,C|A)}}{N_{B,C}} \quad (1)$$

The probabilities can be calculated using relative frequencies that are given by the following relations (Berti et al., 2012; adapted from their Eqs. 2a, 2b, 2c).

$$P(A) \approx N_A \div N_R \quad (2)$$

$$P(B,C) \approx N_{B,C} \div N_R \quad (3)$$

$$P(B,C|A) \approx N_{(B,C|A)} \div N_A \quad (4)$$

where N_R is the total number of days within the debris-flow season; N_A is the total number of debris flows within the study period; $N_{B,C}$ is the total number of joint exceedances of precipitation and temperature percentiles of magnitude B and C within the debris-flow season during the study period; and $N_{(B,C|A)}$ is the number of days with joint exceedances of precipitation and temperature percentiles of magnitude B and C for which a debris flow was observed.

2.3. *Grosswetterlagen* and empirical orthogonal functions

The combination of precipitation and temperature quantiles that have the highest probability to coincide with observed debris flows were then used to select the moments within the simulated data that were in turn subjected to EOF analysis. The EOFs were derived from the MSLP composites of these particular occurrences. The first five eigenvectors (EOFs) with the highest corresponding eigenvalues were retained for further analysis because these together explain ~80% of variability in the data. These EOFs could then be compared to the MSLP anomaly charts by *Grosswetterlagen* index from Cawley (2002) so as to attribute *Grosswetterlagen* types to each EOF.

The *Grosswetterlagen* catalogue for Europe (as reported in Gerstengarbe and Werner, 2005) classifies all days between 1881 and 2004 into a few typical large-scale air-flow patterns. These patterns are further classified according to circulation type and principal flow regimes (i.e., westerly flows belong to the zonal circulation type). By coupling the debris-flow database with the *Grosswetterlagen* catalogue, the typical meteorological situations during observed debris flows could be identified and the principal air-flow directions could be deduced and compared with the calculated EOFs.

3. Results

3.1. Two-dimensional Bayesian probabilities

From the variables considered in this study, extreme precipitation events are the main trigger of debris flows in the Zermatt valley and for the period covered by observational records. Fig. 2 shows that the probability of observing a debris-flow event whilst also observing various combinations of precipitation and temperature magnitudes ($P(A|B,C)$) is highest for the exceedances of the most extreme precipitation percentiles (95th and 99th). By contrast, probabilities for precipitation lower than the 90th percentile remain significantly lower and are therefore not retained for further analysis. Fig. 2 also suggests a positive relationship between the temperature quantiles and ($P(A|B,C)$); however, this is not corroborated by the marginal probabilities and likelihoods shown in Fig. 3. The

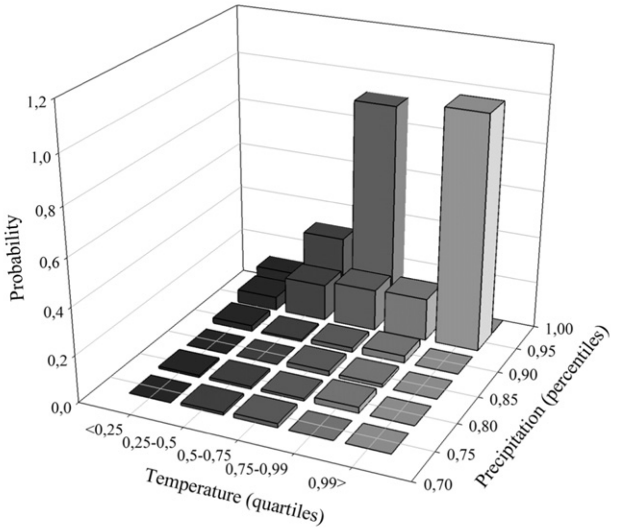

Fig. 2. Probability of observing a debris flow whilst also observing combinations of precipitation and temperature quantiles of various magnitudes.

marginal probability ($P(B,C)$) is the probability of observing a joint exceedance of the precipitation and temperature percentiles and corresponds to the relative frequency distribution. The likelihood ($P(B,C|A)$) is the probability of observing the joint exceedance of the given precipitation and temperature percentiles when a debris flow occurs. As Eq. (1) depicts, the ratio of $P(B,C|A)$ and $P(B,C)$ multiplied by the prior probability $P(A)$ gives the posterior debris-flow probability ($P(A|B,C)$). Because $P(A)$ remains constant, the difference between marginal probability and likelihood indicates high debris-flow probability. However, it is also a measure of the significance of the variables in question because, if the joint exceedance of the precipitation and temperature magnitudes would be irrelevant to the occurrence of debris flows, $P(B,C)$ and $P(B,C|A)$ would be comparable (B would be randomly related with A). Fig. 3 shows that the $P(B,C|A)$ graph reduces significantly for the highest temperature quantiles; whereas the $P(A|B,C)$ graph, shown in Fig. 2, increases for these same quantiles. This means that the increase in posterior probability for these quantiles is the result of a decrease in the total number of joint exceedances of high precipitation and high temperature percentiles ($N_{B,C}$). These combinations of precipitation and temperature percentiles are interesting because of their high probability of coincidence with debris flows but not reliable enough for further interpretation because of their low significance. This analysis indicates that precipitation events exceeding the 95th precipitation percentile in combination with temperatures between the 25th and 75th temperature percentiles have the highest probability to trigger debris flows.

The probabilities for several combinations of the 95th precipitation percentile and temperature percentiles as well as the frequency of exceedance of the given precipitation and temperature percentiles in the HIRHAM simulations are given in Table 1. The HC1 column represents the exceedance of the joint percentiles in the control simulation with the percentile values calculated on the basis of the same control simulation data (for the months between May and October). The HS1/HC1 column represents the future period under the hypothesis of slow adaptation to climate change. In this scenario, the frequency of exceedance of joint percentiles has been calculated for the future, using threshold percentile values that were calculated on the basis of the control simulation data (i.e., temperature and precipitation values were calculated using HC1 simulated data). The HS1/HS1 column represents the future period under the hypothesis of rapid adaptation to climate change, where the frequency of exceedance of the joint percentiles was calculated using threshold percentile values on the basis of the HS1 simulated data. The 95th precipitation percentile and the 30th temperature percentile have been retained for further analysis because this combination satisfies the requirements of high probability and a sufficient number of events required for the calculation of EOFs.

3.2. Synoptic conditions conducive to debris-flow triggering

The types of weather conditions for 102 of the 119 debris-flow events found in the database have been matched to corresponding ones found in the *Grosswetterlagen* catalogue; 14 events occurred outside the period covered by the catalogue (1881–2004) and 3 events within this period had to be listed as *unclassifiable*. Fig. 4 shows the frequency of occurrence of each *Grosswetterlagen* type for days with precipitation quantities that exceeded the 95th precipitation percentile. The West European Trough (TRW) coincides most often with debris flows that occurred during extreme precipitation events. Moreover, this circulation type typically coincides with debris-flow triggering during summer months (June, July, and August). The Central European Ridge (BM), West Cyclonic situation (Wz), and British Isles Low (TB) all coincide equally often with observed debris flows and extreme precipitation events. From the classification (Table 2, Appendix A), one can presume that these *Grosswetterlagen* types correspond to southerly flows (TRW and TB), situations with weak horizontal pressure gradients over Europe (BM) and/or westerly flows (Wz). Fig. 5 shows the result of the classification of all *Grosswetterlagen* types into principal air-flow directions. Southerly flows, weak horizontal pressure gradients (HD), and westerly flows are distinctly the situations that are most conducive to debris-flow triggering.

The first three EOFs for the control and future period simulations are given in Fig. 6. The EOFs were compared with the MSLP anomaly charts by *Grosswetterlagen* indices (Cawley, 2002), which allowed allocation of a *Grosswetterlagen* type to each EOF. The first EOF of the control

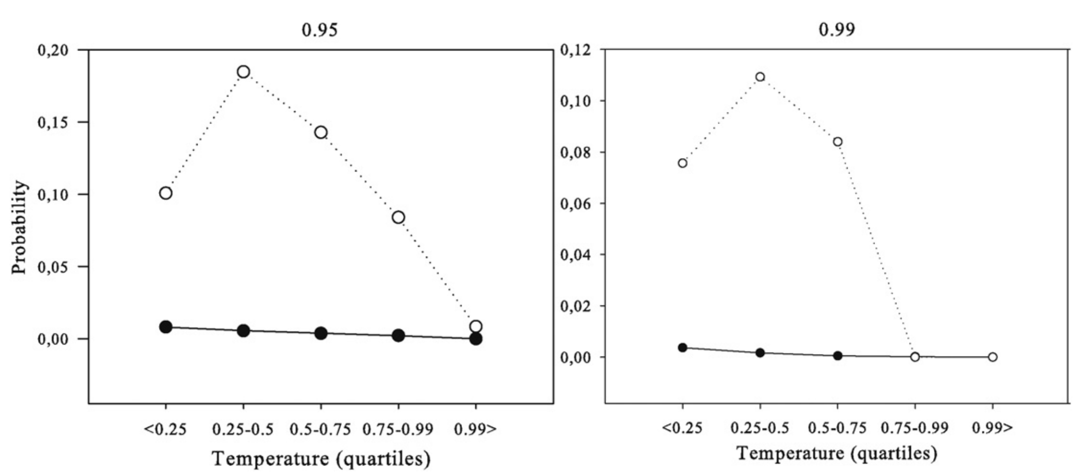

Fig. 3. Marginal probabilities and likelihoods of observing a precipitation event of the 95th and 99th percentiles in combination with various temperature magnitudes.

Table 1
Cumulative frequency of joint exceedances of precipitation and temperature percentiles in observed data (with associated probabilities) and in the HIRHAM simulations for the control and future periods.

Precipitation percentile	Temperature percentile	Observed (#)	P(A |B,C)	HC1 (#)	HS1/HC1 (#)	HS1/HS1 (#)
0.95	0.05	553	0.16	215	215	155
	0.1	489	0.18	200	208	134
	0.15	427	0.19	163	186	118
	0.2	374	0.20	139	176	102
	0.25	335	0.21	125	166	90
	0.3	286	0.22	113	156	78
	0.35	254	0.22	102	146	69
	0.4	214	0.23	83	139	47
	0.45	186	0.22	65	129	38
	0.5	165	0.23	53	118	30
	0.55	150	0.21	40	111	22
	0.6	132	0.21	30	99	16
	0.65	103	0.18	20	84	8
	0.7	76	0.16	15	75	6
	0.75	60	0.18	7	52	5
	0.8	44	0.25	3	40	3
	0.85	29	0.20	3	30	2
	0.9	21	0.24	2	21	2
	0.95	8	0.13	0	9	1
	0.99	1	1.00	0	3	0

simulation corresponds well to the Central European Ridge (BM), with low pressure gradients over Europe. This *Grosswetterlagen* type coincides well with observed debris flows and extreme precipitation events. The second EOF resembles a Western Cyclonic situation (Wz) while shifted to the east. In this type of situation, the relatively low pressure area over Scandinavia and the higher pressure area over southeastern Europe induce southwesterly flows advecting moisture from the Atlantic toward the Alps. The third EOF resembles the South Anticyclonic (Sa) pattern during which the low pressure over the British Isles and the relatively high pressure area over eastern Europe induce a southerly flow that directs warm and humid air masses to the Alps. The second column in Fig. 6 shows the first three EOFs for the future period under the hypothesis of slow adaptation to climate change. This means that all events in the HIRHAM simulation for the future period exceeding the 95th precipitation percentile and the 30th temperature percentile calculated on the basis of the HIRHAM simulation of the current (control) period have been used for the EOF calculation. The first EOF is similar to the West Cyclonic (Wz) *Grosswetterlage*, which induces westerly flows. The second EOF matches the South Anticyclonic (Sa) situation and the third may correspond to the South East Cyclonic (SEz) situation. Finally, the third column in Fig. 6 shows the first three EOFs for the HIRHAM simulation of

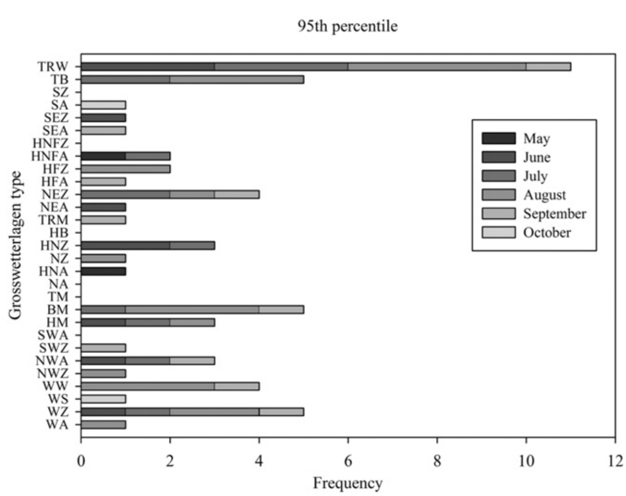

Fig. 4. Frequency of coincidence of *Grosswetterlagen* types with observed debris flows for the period 1881–2004 for days that exceeded the 95th precipitation percentile.

the future climate under the hypothesis of a slow adaptation to climate change. The first EOF is similar to the South-West Cyclonic (SWz) *Grosswetterlage*. The pressure distributions in these types of situations induce southwesterly flows. The second EOF explains almost as much of the MSLP variability as the first EOF and resembles a situation of weak horizontal pressure gradients over Europe. The third EOF matches the South East Cyclonic situation. For all simulations, the fourth and fifth EOFs were similar and represented the West cyclonic (Wz) situation and the West European Trough (TRW).

Fig. 7 shows the result of the classification of all EOFs of the three simulations into principal air-flow directions. The control simulation captures rather well the principal flow directions; weak horizontal pressure gradients (HP), westerly and southerly flows being the most important situations conducive to the precipitation and temperature conditions most likely to trigger debris flows in the Zermatt valley. Under the climate change scenario with slow adaptation, weak horizontal pressure gradients disappear completely in favour of westerly and southerly flows; southeasterly flows are also introduced. Under the hypothesis of climate change with rapid adaptation, weak horizontal pressure gradients are reintroduced, though south/south-westerly flows remain the most important directions. As is the case for the rapid climate change scenario, southeasterly flows gain in importance.

4. Discussion

This study addresses the types of meteorological situations conducive to the precipitation and temperature conditions most likely to trigger debris flows in the Zermatt valley under current and future climates. Though precipitation and temperature are the main debris-flow triggers, other nonmeteorological factors such as the presence of permafrost, snow cover, vegetation, and ground characteristics also influence triggering; these factors are in turn affected by climate change. Because this study focuses on the meteorological factors only, it expresses debris-flow triggering in terms of probabilities.

The two-dimensional Bayesian analysis used in this study allows for the use of two or more variables in the probability calculation as well as for the evaluation of the significance of each variable. As such, we established precipitation as the main debris-flow trigger. Precipitation quantities exceeding the 95th precipitation percentile have a significantly higher probability to trigger debris flows. Results also indicate that a certain temperature range rather than extreme temperatures has a higher probability to coincide with observed debris flows. The low probabilities for the lower temperatures reflect the fact that precipitation may fall in a solid form at these temperatures. As the meteorological station of Grächen is located below the source areas of debris flows, measured temperatures below +5 °C are likely to be associated with precipitation falling in solid form in the source areas and thus not trigger debris flows (Stoffel et al., 2005, 2014b; Stoffel, 2010). The low probabilities for high temperature percentiles may be explained by the circulation types observed during extreme precipitation events. The coupling of the *Grosswetterlagen* catalogue with the debris-flow database (Bollschweiler and Stoffel, 2010a) indicated that southerly flows, weak horizontal pressure gradients over Europe, and westerly flows were mostly associated with debris-flow triggering in the Zermatt valley. Westerly flows in summer bring relatively cooler air from the Atlantic in the direction of the Alps and rainstorms typically form in the cold front of depressions (MétéoSuisse, 2013). The moisture advected by southerly flows is forced to rise over the Alps, causing the air temperature to drop, which then results in sustained precipitation.

In contrast to this study, the studies of Jomelli et al. (2009) and Damm and Felderer (2013) found that higher temperatures do have an important influence on debris-flow frequency in the French and Italian Alps. The reason for this is that temperature influences debris availability through permafrost degradation and glacier recession in these otherwise debris-limited areas. The Bayesian probability calculation

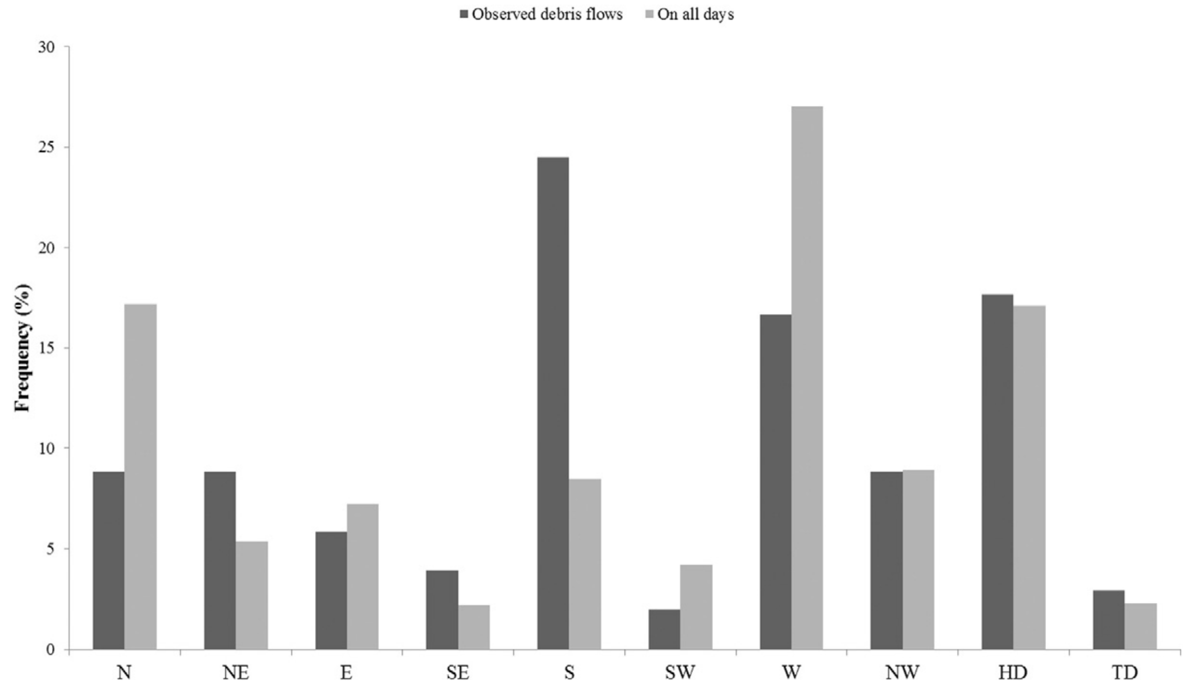

Fig. 5. Principal air-flow directions as well as situations with high pressure systems (HD) and low pressure systems (TD) over Europe on days for which debris flows were observed.

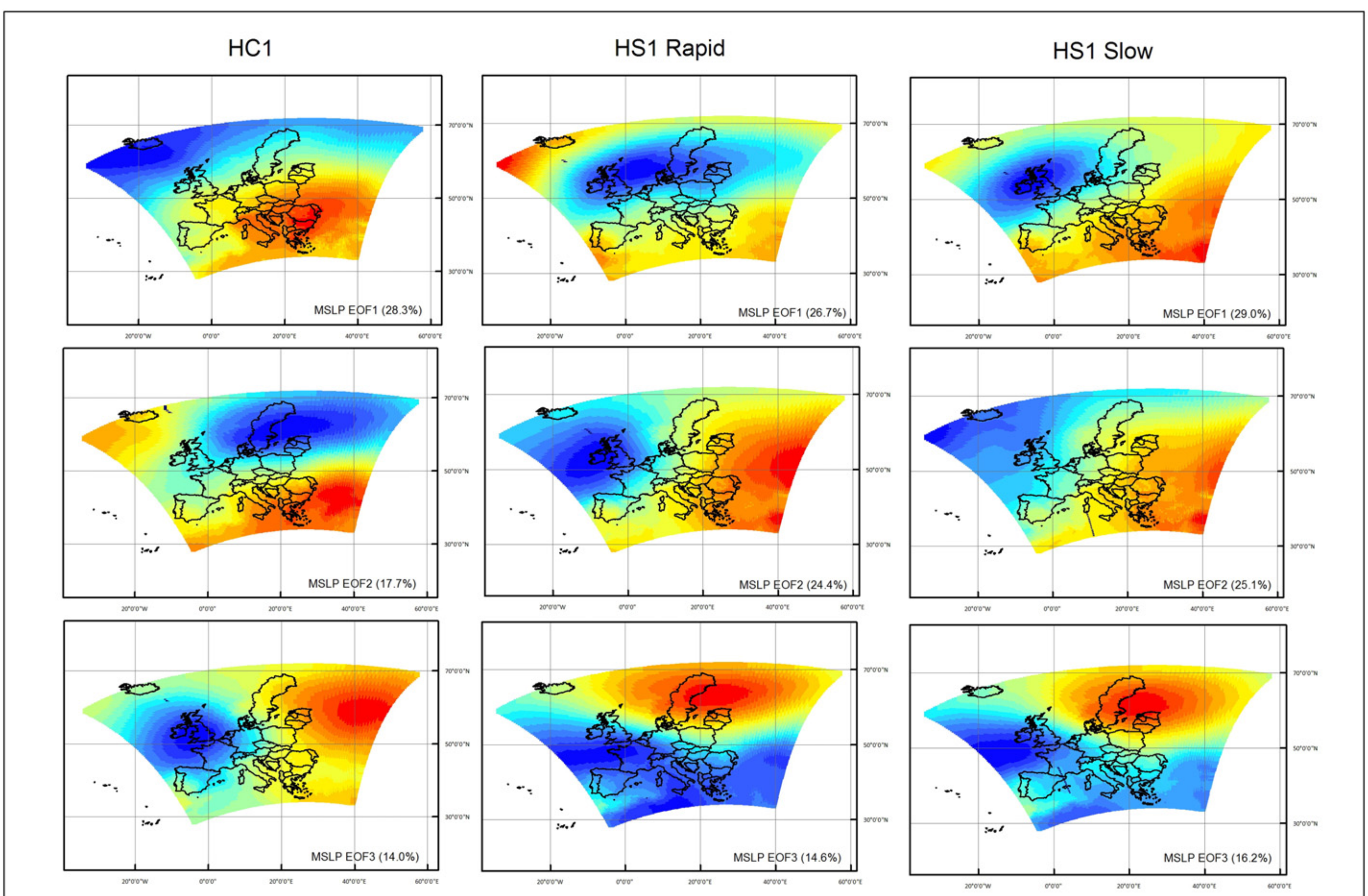

Fig. 6. First three empirical orthogonal functions (EOFs) for the HIRHAM control period (HC1), the future period under the hypothesis of slow adaptation to climate change (HS1/HC1), and the future period under the hypothesis of rapid adaptation to climate change (HS1/HS1). For each EOF the percentage of explained total variance is given. Scale values of the EOFs are given in Appendix B. The visualisation of the EOFs was carried out in ArcMap. The European boundaries layer was adapted from: GISCO — Eurostat (European Commission) Administrative boundaries: © EuroGeographics, UN-FAO, Turkstat.

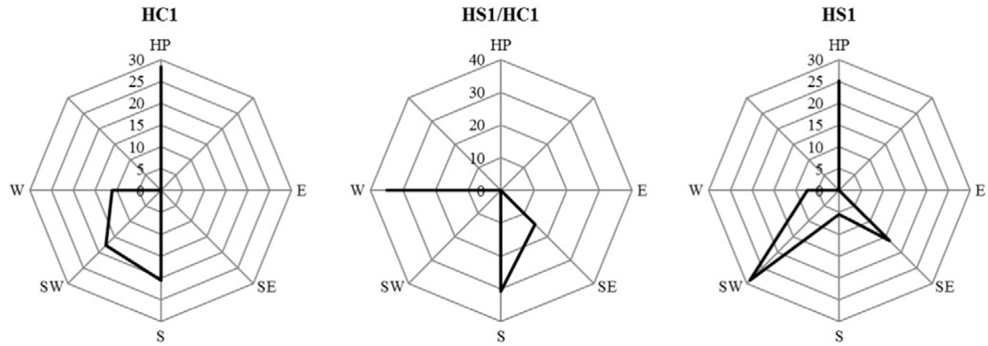

Fig. 7. The principal flow directions (in terms of the percentage of total variance explained by each EOF) for events exceeding the 95th precipitation percentile and the 30th temperature percentile for the HIRHAM control and future simulations.

used in this study would allow for better quantification of the influence of temperature on debris-flow triggering in these areas.

The choice to retain the 95th precipitation percentile and the 30th temperature percentile for further analysis was based on high probability, high significance, and a sufficient number of events in the HIRHAM simulations. For example, the combination of percentiles $P_{99}T_{50-75}$, with a probability of 0.91 based on 10 debris-flow events for 11 joint precipitation and temperature percentiles, could not be retained for further analysis because of its low significance and insufficient occurrence in the HIRHAM simulations. However, it would be appropriate to monitor the occurrence of these types of conditions in the future.

This analysis is based on the results of the HIRHAM control and simulation model runs with the IPCC A2 emissions scenario. New scenarios or representative concentration pathways (RCPs) were formulated based on additional variables such as land use and to better suit the more detailed information requirements of current climate models (Van Vuuren et al., 2011). This study is based on the older but well-established SRES scenarios and as such, the results of this study should be viewed in this context.

While using the two-dimensional Bayesian probability calculation, we must keep in mind that this approach is based on prior and marginal probabilities. This means that if data and measurements do not contain a debris flow triggered by a certain amount of rainfall, this will result in zero probability for this type of rainfall event. The long data set used for this study as well as the continued updating of data sets with new debris-flow events mitigates this problem. Furthermore, like other methods, the Bayesian probability calculation is based on past debris-flow events. This means that using past probabilities for projection in the future can only be done under the hypothesis that other variables are fixed. And finally, probabilities depend also on the size of the study area; the greater the area, the higher the probability of debris flows occurring (Berti et al., 2012). For comparison, keep in mind that this study is based on multiple torrents in the Zermatt valley. Where precipitation and temperature measurements are concerned, the meteorological station of Grächen is not located within the source area. As such, measured temperatures and rainfall quantities may not be representative. The use of percentiles rather than exact rainfall sums has mitigated this problem.

The coupling of the *Grosswetterlagen* catalogue with the debris-flow database indicated that the West European Trough (TRW) coincided most with observed debris flows that were triggered by precipitation quantities that exceeded the 95th precipitation percentile. The Central European Ridge (BM), the West Cyclonic situation (Wz), the British Isles Low (TB), and the North Eastern Cyclonic (Nez) also coincided frequently with observed debris flows. These could be further classified into southerly flows, situations of weak horizontal pressure gradients over Europe, and westerly flows. These results are partly in accordance with the findings of previous studies: Attinger and Fallot (2003) identified the West European Trough, the West Cyclonic situation, the British Isles Low, South Anticyclonic (Sa), Norwegian Sea–Fennoscandian High Cyclonic (HNFZ), and South-East Cyclonic (SEz) as the principal *Grosswetterlagen* causing precipitation events of 100 mm and more in the Valais. Courvoisier (1981) also identified westerly flows and situations with weak horizontal pressure gradients over Europe as types of situations causing high precipitation quantities in Switzerland. These results formed a basis to compare with the EOFs calculated on the HIRHAM simulation data.

The first five EOFs from the HIRHAM control period were identified as the Central European Ridge (BM), the West Cyclonic situation (Wz) (second and fourth EOF), the South Anticyclonic situation (Sa), and the West European Trough (TRW). These are the same types of situations that were identified for the observed debris flows. Interestingly enough, the West European Trough was the most important *Grosswetterlage* for the observed debris flows and is represented only by the fifth EOF. A possible explanation for this is the overrepresentation of high temperature events in the selection; all dates exceeding the 95th precipitation percentile and the 30th temperature percentile were used, whereas in the observed data high temperature percentiles did not have a high probability to trigger debris flows. However, the translation of *Grosswetterlagen* into principal flow directions did yield more comparable results. As such, the HIRHAM model represents the principal air-flow directions responsible for the precipitation and temperature conditions most likely to trigger debris flows in the observed data quite well.

Under the hypothesis of slow adaptation to climate change, other variables such as ground and vegetation characteristics have not yet responded to changing climatic conditions. This entails that for this scenario we used the same percentile thresholds of the HIRHAM current climate simulation for the future climate. Mostly the same *Grosswetterlagen* were identified for the slow adaptation to climate change scenario as for the control simulation. The South East Cyclonic situation was introduced; this type of situation leads to southeasterly flows but was also one of the situations identified by Attinger and Fallot (2003). Furthermore, westerly and southerly flows gain in importance at the expense of situations with weak horizontal pressure gradients.

Under the hypothesis of a rapid adaptation of ground and vegetation characteristics to climate change, higher temperatures may allow vegetation to migrate to higher altitudes and in turn might decrease slope instability and reduce the availability of sediment in the source areas of debris flows. The complete disappearance of permafrost may also influence these variables. The rapid adaptation to climate change scenario assumes that only extreme precipitation events will lead to debris-flow triggering

Table 2
Classification of Grosswetterlagen types into air-flow directions.

Circulation type	Flow direction	# events	Grosswetterlagen types	Mean T (°C)
Meridional	N	9	NA, HNA, NZ, HNZ, HB, TRM	7.81
|	NE	9	NEA, NEZ	9.62
|	E	6	HFA, HFZ, HNFA, HNFZ	10.24
|	SE	4	SEA, SEZ	9.28
|	S	25	SA, SZ, TB, TRW	10.15
Mixed	SW	2	SWZ, SWA	11.15
Zonal	W	17	WA, WZ, WS, WW	9.76
Mixed	NW	9	NWZ, NWA	8.55
|	HD	18	HM, BM,	12.28
|	TD	3	TM	11.03

in a future climate. As such, events have been selected using percentile thresholds calculated on the basis of data from simulations of the future climate. Situations of weak horizontal pressure gradients over Europe regain in importance in the scenario of rapid adaptation. The importance of westerly flows decreases, whereas south/southwesterly flows gain in importance and southeasterlies are also introduced.

This exploratory analysis using EOFs calculated for various simulations is useful, and spatial patterns are reasonably comparable to *Grosswetterlagen* known to cause extreme precipitation in the Valais. Both future scenarios indicate an increase in southerly flows and in southeasterlies. In the scenario of rapid adaptation to climate change, this is at the expense of westerly flows, which is comparable to findings by Rohrer (2013). Situations of weak horizontal pressure gradients disappear in the slow adaptation to climate change scenario and become almost equally important as in the control simulation for the scenario of rapid adaptation to climate change. A possible explanation for this is that the convective precipitation typical during these situations requires relatively high temperatures in the low levels above the surface. Events for the slow adaptation scenario have been selected using the control period data, thus situations with relatively low temperatures were included in the EOF calculation. As such, events representing weak horizontal pressure gradients may have been crowded out by events with lower temperature values.

The calculation of EOFs is a well-established technique in atmospheric research. However, the physical interpretability of EOFs is still subject to controversy. In line with the mode of interpretation of EOFs put forward by Behera et al. (2003), this study has referred to the composites that were used for the calculation of EOFs and associated the results with Cawley's MSLP anomaly charts (2002) for validation.

5. Conclusions

The objective of this study was to find what types of meteorological situations are conducive to the precipitation and temperature conditions that are most likely to cause debris-flow triggering in current and future climates. The two-dimensional Bayesian probability calculation was introduced as a means to take into account uncertainties caused by other than meteorological variables. We found that precipitation quantities exceeding the 95th precipitation percentile had a significantly higher probability to coincide with debris flows. No such relationship was found for temperature percentiles. Southerly air flows, weak horizontal pressure gradients over Europe, and westerly flows were mostly responsible for precipitation quantities exceeding the 95th precipitation percentile and debris-flow triggering in the Zermatt valley.

Using data from the HIRHAM model under the IPCC A2 emission scenario, this study investigated whether in future climates the same large-scale meteorological situations will be responsible for the precipitation and temperature conditions likely to trigger debris flows. We found that though the EOFs resulting from the simulations were fairly comparable to the *Grosswetterlagen* known to cause high precipitation quantities in the Valais, the most important *Grosswetterlage* from the observations (TRW) was represented by the fifth EOF calculated for the control simulation. When these *Grosswetterlagen* were translated into principal airflow directions however, the results for the control simulation did correspond to observations. In a climate change scenario with slow adaptation, precipitation and temperature conditions prone to debris-flow triggering will occur more often because of southerly and westerly air flows, whereas situations with weak pressure gradients will fade out. In a climate change scenario with rapid adaptation, southerly flows and weak pressure gradients over Europe will more often favour these types of conditions. Both scenarios introduce southeasterly flows.

Acknowledgements

The authors gratefully acknowledge access to and use of climate model output from the EU-FP5 PRUDENCE project. We also thank the reviewers and guest editors for their insightful comments and suggestions which have improved the readability, clarity and overall quality of this work.

Appendix A

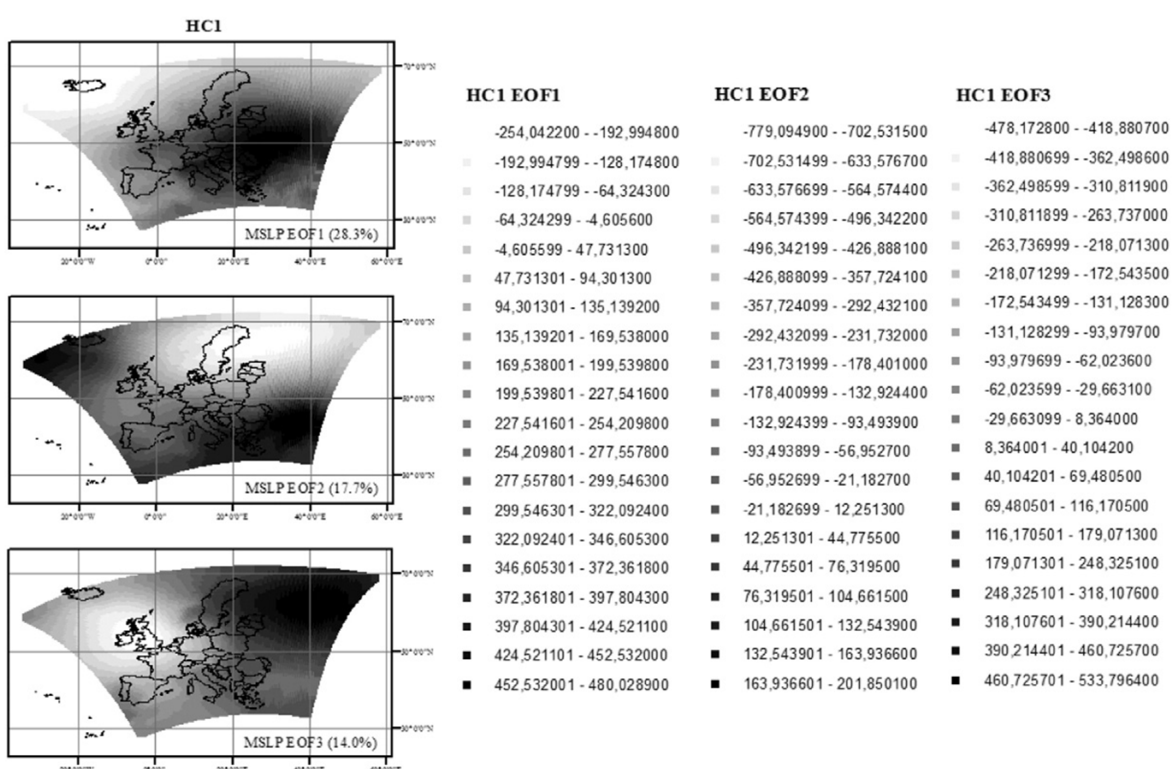

Fig. 8. First three empirical orthogonal functions (EOFs) for the HIRHAM control period (HC1). For each EOF, the percentages of explained total variance and scale values are given.

Appendix B

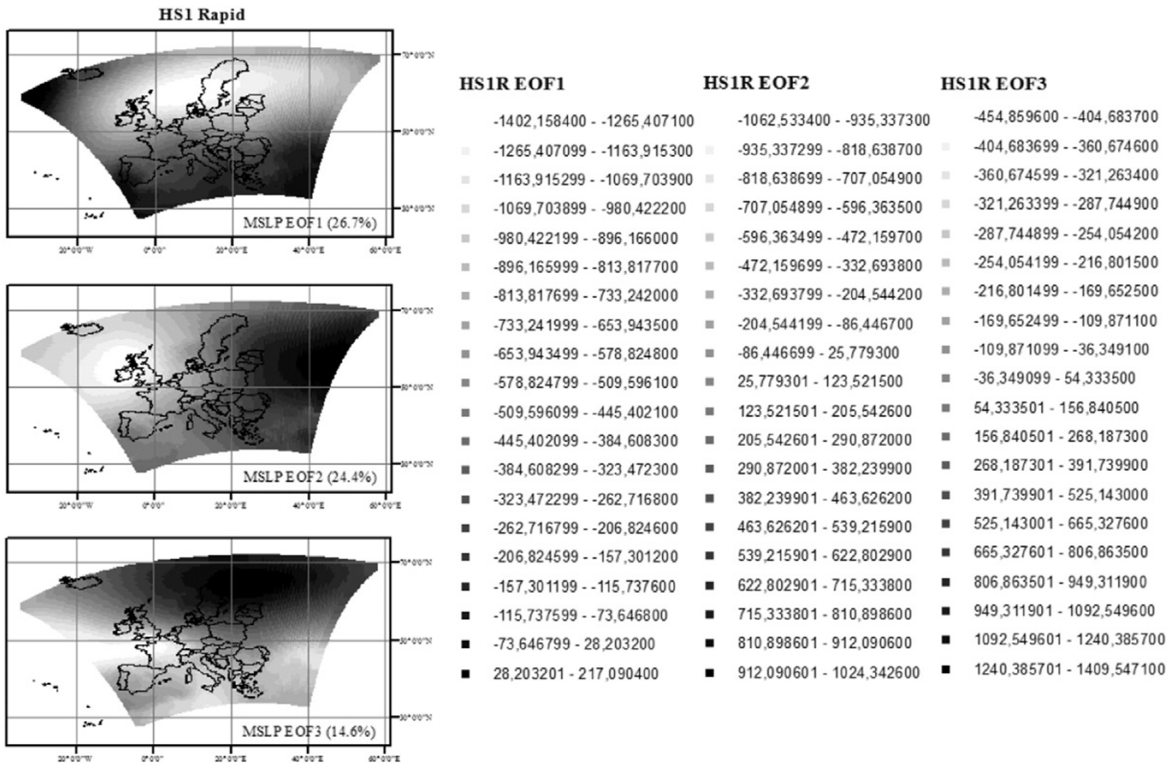

Fig. 9. First three empirical orthogonal functions (EOFs) for the HIRHAM future period under the hypothesis of rapid adaptation to climate change. For each EOF, the percentages of explained total variance and scale values are given.

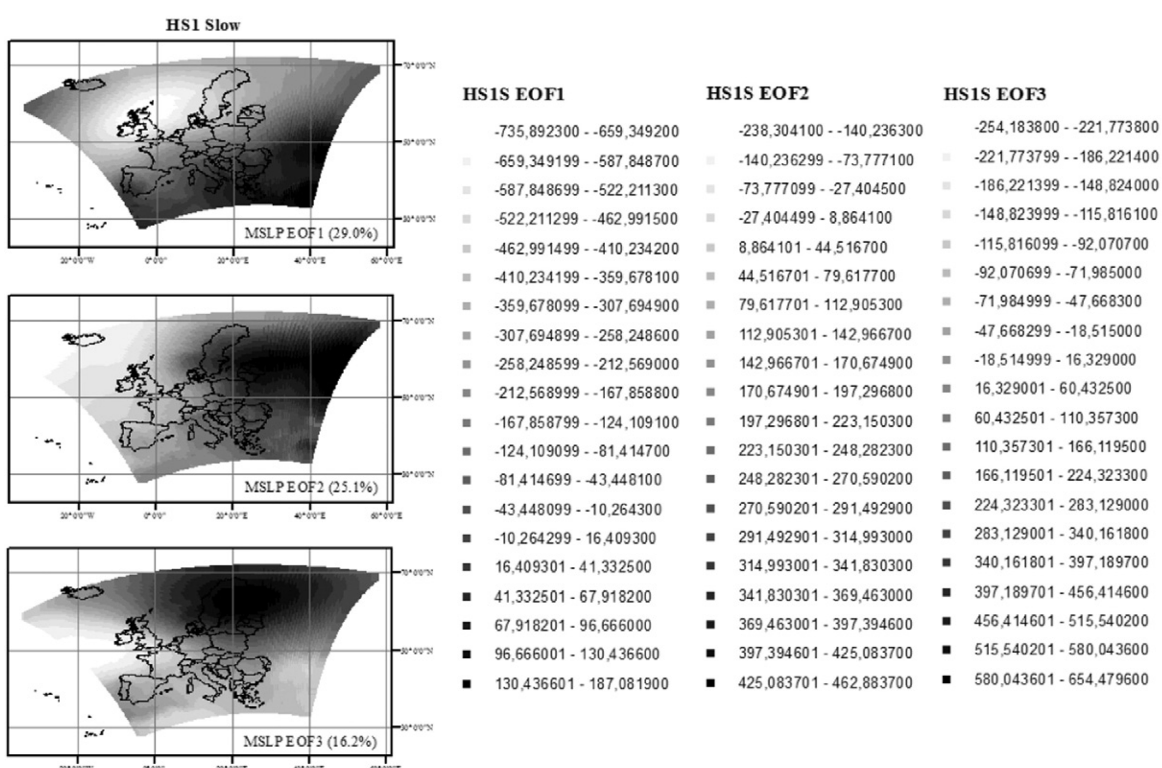

Fig. 10. First three empirical orthogonal functions (EOFs) for the HIRHAM future period under the hypothesis of slow adaptation to climate change. For each EOF, the percentages of explained total variance and scale values are given.

References

Attinger, S., Fallot, J.M., 2003. Fréquence des intempéries et des précipitations abondantes en Valais (Alpes Suisses Occidentales) durant le 20ieme siècle. Publications de l'Association Internationale de Climatologie (http://www.climato.be/aic/colloques/actes/PubAIC/art_2003_vol15/Article%2031%20S%20Attinger.pdf. Accessed 19 March 2014).

Behera, S.K., Rao, S.A., Saji, H.N., Yamagata, T., 2003. Comments on "a cautionary note on the interpretation of Eofs". J. Clim. 16, 1087–1093.

Beniston, M., 2009. Trends in joint quantiles of temperature and precipitation in Europe since 1901 and projected for 2100. Geophys. Res. Lett. 36, L07707.

Beniston, M., Goyette, S., 2007. Changes in variability and persistence of climate in Switzerland: exploring 20th century observations and 21st century simulations. Glob. Planet. Chang. 57, 1–15.

Beniston, M., Keller, F., Goyette, S., 2003. Snow pack in the Swiss Alps under changing climatic conditions: an empirical approach for climate impact studies. Theor. Appl. Climatol. 74, 19–31.

Beniston, M., Stephenson, D.B., Christensen, O.B., Ferro, C.A.T., Frei, C., Goyette, S., Halsnaes, K., Holt, T., Jylhä, K., Koffi, B., Palutikof, J., Schöll, R., Semmler, T., Woth, K., 2007. Future extreme events in European climate: an exploration of Regional Climate Model projections. Clim. Chang. 81, 71–95.

Berti, M., Martina, M.L.V., Franceschini, S., Pignone, S., Simoni, A., Pizziolo, M., 2012. Probabilistic rainfall thresholds for landslide occurrence using a Bayesian approach. J. Geophys. Res. Earth Surf. 117, F04006.

Bollschweiler, M., Stoffel, M., 2010a. Changes and trends in debris-flow frequency since AD 1850: results from the Swiss Alps. Holocene 20, 907–916.

Bollschweiler, M., Stoffel, M., 2010b. Tree rings and debris flows: recent developments, future directions. Prog. Phys. Geogr. 34, 625–645.

Borga, M., Stoffel, M., Marchi, L., Marra, F., Jakob, M., 2014. Hydrogeomorphic response to extreme rainfall in headwater systems: Flash floods and debris flows. J. Hydrol. 518, 194–205.

Cawley, G.C., 2002. Mean daily Surface Level Pressure anomaly charts by Grosswetterlagen index. University of East Anglia (http://theoval.cmp.uea.ac.uk/~gcc/projects/accord/experiments/experiment1a/report.html. Accessed 24 October 2013).

Christensen, J.H., 2004. Prediction of Regional scenarios and Uncertainties for Defining European Climate change risks and Effects. (Prudence. http://prudence.dmi.dk. Accessed 8 April 2014).

Christensen, J.H., Christensen, O.B., 2003. Climate modelling: severe summertime flooding in Europe. Nature 421, 805–806.

Christensen, J.H., Christensen, O.B., 2007. A summary of the Prudence model projections of changes in European climate by the end of this century. Clim. Chang. 81, 7–30.

Courvoisier, H.W., 1981. Starkniederschläge in der Schweiz in abhängigkeit vom druck-, temperatur- und feuchtefeld. Veröffentlichungen der Schweizerischen Meteorologischen Anstallt. (http://www.meteoswiss.admin.ch/web/de/forschung/publikationen/alle_publikationen/abgabgeschloss_hoehentiefs.Par.0001.DownloadFile.tmp/veroeff45.pdf. Accessed 19 March 2014).

Damm, B., Felderer, A., 2013. Impact of atmospheric warming on permafrost degradation and debris flow initiation — a case study from the eastern European Alps. Quat. Sci. J. 62, 136–149.

Emori, S., Brown, S.J., 2005. Dynamic and thermodynamic changes in mean and extreme precipitation under changed climate. Geophys. Res. Lett. 32, L17706.

Fischer, E.M., Beyerle, U., Knutti, R., 2013. Robust spatially aggregated projections of climate extremes. Nat. Clim. Chang. 3, 1033–1038.

Gerstengarbe, F.W., Werner, P.C., 2005. Katalog der Grosswetterlagen Europas (1881–2004) nach Paul Hess und Helmut Brezowsky 6, verbesserte und ergänzte auflage. Report Potsdam Institute for Climate Impact Research (https://www.pik-potsdam.de/research/publications/pikreports/.files/pr100.pdf. Accessed 19 March 2014).

Gobiet, A., Kotlarski, S., Beniston, M., Heinrich, G., Rajczak, J., Stoffel, M., 2014. 21st century climate change in the European Alps — a review. Sci. Total Environ. 493, 1138–1151.

IPCC, 2012. Managing the risks of extreme events and disasters to advance climate change adaptation. In: Field, C.B., Barros, V., Stocker, T.F., Qin, D., Dokken, D.J., Ebi, K.I., Mastrandrea, M.D., Mach, K.J., Plattner, G.-K., Allen, S.K., Tignor, M., Midgley, P.M. (Eds.), A special report of working groups I and II of the intergovernmental panel on climate change. Cambridge University Press, Cambridge, United Kingdom and New York, NY, USA.

IPCC, 2013. Summary for Policymakers. In: Stocker, T.F., Qin, D., Plattner, G.K., Tignor, M., Allen, S.K., Boschung, J., Nauels, A., Xia, Bex, V., Midgley, P.M. (Eds.), Climate Change 2013: The Physical Science Basis. Contribution of Working Group I to the Fifth Assessment Report of the Intergovernmental Panel on Climate Change. Cambridge University Press, Cambridge, United Kingdom and New York, NY, USA, pp. 2–14.

Iverson, R.M., Reid, M.E., LaHusen, R.G., 1997. Debris-flow mobilization from landslides. Annu. Rev. Earth 85–138 (Pl Sc 25).

Jakob, M., 1996. Morphometric and Geotechnical controls of debris-flow frequency and magnitude in Southwestern British Columbia. Department of GeographyUniversity of British Columbia, Vancouver (242 pp.).

Jakob, M., Hungr, O., 2005. Debris-flow hazards and related phenomena. Springer, Berlin Heidelberg (739 pp.).

Jakob, M., Stein, D., Ulmi, M., 2011. Vulnerability of buildings to debris flow impact. Nat. Hazards 60, 241–261.

Jomelli, V., Brunstein, D., Déqué, M., Vrac, M., Grancher, D., 2009. Impacts of future climatic change (2070–2099) on the potential occurrence of debris flows: a case study in the Massif Des Ecrins (French Alps). Clim. Chang. 97, 171–191.

Jonkman, S.N., 2005. Global perspectives on loss of human life caused by floods. Nat. Hazards 34, 151–175.

Kharin, V., Zwiers, F., Zhang, X., Hegerl, G., 2007. Changes in temperature and precipitation extremes in the IPCC ensemble of global coupled model simulations. J. Clim. 20, 1419–1444.

Kyselý, J., Beranovà, R., 2009. Climate-change effects on extreme precipitation in Central Europe: uncertainties of scenarios based on regional climate models. Theor. Appl. Climatol. 95, 361–374.

Lenderink, G., van Meijgaard, E., 2008. Increase in hourly precipitation extremes beyond expectations from temperature changes. Nat. Geosci. 1, 511–514.

Lugon, R., Stoffel, M., 2010. Rock-glacier dynamics and magnitude-frequency relations of debris flows in a high-elevation watershed: Ritigraben, Swiss Alps. Glob. Planet. Chang. 73, 202–210.

MétéoSuisse, 2013. Situations Météorologiques typiques dans la région des Alpes. Ed. Office fédéral de météorologie et de climatologie and Winterthur Assurances (Zürich). http://www.meteoschweiz.admin.ch/medialib/documents/fr/broschueren.Par.0001.File.tmt/brochure.pdf (Accessed 19 March 2014).

Nikolopoulos, E., Borga, M., Marra, F., Crema, S., Marchi, L., 2015. Debris flows in the eastern Italian Alps: seasonality and atmospheric circulation patterns. Nat. Hazards Earth Syst. Sci. 15, 647–656.

Pall, P., Allen, M.R., Stone, D.A., 2007. Testing the Clausius–Clapeyron constraint on changes in extreme precipitation under CO_2 warming. Clim. Dyn. 28, 351–363.

Qian, B., Corte-Real, J., Xu, H., 2000. Is the North Atlantic oscillation the most important atmospheric pattern for precipitation in Europe? J. Geophys. Res. 105, 11,901–11,910.

Rajczak, J., Pall, P., Schär, C., 2013. Projections of extreme precipitation events in regional climate simulations for Europe and the Alpine Region. J. Geophys. Res. 118, 3610–3626.

Rohrer, M., 2013. Climate change and circulation types in the Alpine region. MeteoSwiss Federal Office of Meteorology and Climatology (http://www.meteoschweiz.admin.ch/web/de/forschung/publikationen/alle_publikationen/SR91_Rohrer.Par.0001.DownloadFile.tmp/sr91rohrer.pdf. Accessed 19 March 2014).

Sassa, K., 1984. The mechanism starting liquefied landslides and debris flows. Proceedings of the 4th International Symposium on Landslides, pp. 349–354 (Toronto, June 2,).

Schär, C., Lüthi, D., Beyerle, U., 1999. The soil-precipitation feedback: a process study with a regional climate model. J. Clim. 12, 722–741.

Schneuwly-Bollschweiler, M., Stoffel, M., 2012. Hydrometeorological triggers of periglacial debris flows in the Zermatt valley (Switzerland) since 1864. J. Geophys. Res. Earth Surf. 117, F02033.

Seneviratne, S., Lüthi, D., Litschi, M., Schär, C., 2006. Land-atmosphere coupling and climate change in Europe. Nature 443, 205–209.

Stoffel, M., 2010. Magnitude-frequency relationships of debris flows — a case study based on field surveys and tree-ring records. Geomorphology 116, 67–76.

Stoffel, M., Beniston, M., 2006. On the incidence of debris flows from the early little ice age to a future greenhouse climate: a case study from the Swiss alps. Geophys. Res. Lett. 33, L16404.

Stoffel, M., Corona, C., 2014. Dendroecological dating of geomorphic disturbance in trees. Tree-Ring Res. 70, 3–20.

Stoffel, M., Huggel, C., 2012. Effects of climate change on mass movements in mountain environments. Prog. Phys. Geogr. 36, 421–439.

Stoffel, M., Lièvre, I., Conus, D., Grichting, M.A., Raetzo, H., Gärtner, H.W., Monbaron, M., 2005. 400 years of debris flow activity and triggering weather conditions: ritigraben VS, Switzerland. Arct. Antarct. Alp. Res. 37 (3), 387–395.

Stoffel, M., Conus, D., Grichting, M.A., Lièvre, I., Maître, G., 2008. Unraveling the patterns of late Holocene debris-flow activity on a cone in the central Swiss alps: chronology, environment and implications for the future. Glob. Planet. Chang. 60, 222–234.

Stoffel, M., Schneuwly-Bollschweiler, M., Beniston, M., 2011. Rainfall characteristics for periglacial debris flows in the Swiss alps: past incidences-potential future evolutions. Clim. Chang. 105, 263–280.

Stoffel, M., Tiranti, D., Huggel, C., 2014a. Climate change impacts on mass movements – case studies from the European alps. Sci. Total Environ. 493, 1255–1266.

Stoffel, M., Mendlik, T., Schneuwly-Bollschweiler, M., Gobiet, A., 2014b. Possible impacts of climate change on debris-flow activity in the Swiss alps. Clim. Chang. 122, 141–155.

Toreti, A., Schneuwly-Bollschweiler, M., Stoffel, M., Luterbacher, J., 2013. Atmospheric forcing of debris flows in the southern Swiss alps. J. Appl. Meteorol. Climatol. 52, 1554–1560.

Van Vuuren, D.P., Edmonds, J., Kainuma, M., Riahi, K., Thomson, A., Hibbard, K., Hurtt, G.C., Kram, T., Krey, V., Lamarque, J.F., Masui, T., Meinshausen, M., Nakicenovic, N., Smith, S.J., Rose, S.K., 2011. The representative concentration pathways: an overview. Clim. Chang. 109, 5–31.

Wieczorek, G.F., Glade, T., Jakob, M., Hungr, O., 2005. Climatic factors influencing the occurrence of debris flows. Debris-Flow Hazards And Related Phenomena. Springer, Berlin Heidelberg, pp. 325–362.